

# Study on rate azimuth platform inertial navigation system

Cai Tijing<sup>1</sup> G. I. Emeliantsev<sup>2</sup>

(<sup>1</sup>Department of Instrument Science and Technology, Southeast University, Nanjing 210096, China)

(<sup>2</sup>St. Petersburg State Institute of Fine Mechanics and Optics, St. Petersburg 197101, Russia)

**Abstract:** The cost of the gravity passive inertial navigation system will be lower with a rate azimuth platform and gravity sensor constituting a gravity measurement and navigation system. According to the system performance characteristics, we study the rate azimuth platform inertial navigation system (RAPINS), give the system navigation algorithm, error equations of the attitude, velocity and position of the rate azimuth platform, and random error models of the accelerometer and gyro. Using the MATLAB/Simulink tools, we study the RAPINS and RAPINS with velocity damping. Simulation results demonstrate that the RAPINS with velocity damping has small errors in platform attitude and position and satisfies gravity measurement and navigation requirement.

**Key words:** rate azimuth platform; gravimeter; inertial navigation system; gravity passive navigation system

At the beginning of the 1980's some of institutes and universities in China researched the rate azimuth platform inertial navigation system (RAPINS)<sup>[1,2]</sup>. Based on this platform inertial navigation system, RAPINS leaves out the azimuth ring and stabilized loop, uses rate gyro to measure the angular rate of the platform azimuth angle, and then integrates it to determine the platform azimuth angle. Compared with the 3-axis platform inertial navigation system, RAPINS has a simpler configuration, smaller size and better reliability. In the 1990's the strapdown inertial navigation system (SINS) began to be used in China. RAPINS had no advantage, compared with SINS. Therefore the project of RAPINS stopped. In the last decade, a new important navigation technique — gravity passive inertial navigation system attracted military attention in big countries. In the 1990's, America's Lockheed Martin Naval Electronics and Surveillance Systems developed a gravity passive navigation system<sup>[3,4]</sup>, which included inertial navigator module, universal gravity module, precision navigator module and terrain estimation module. The gravity passive navigation was demonstrated during 1998 and 1999. The goal of this exercise was to show that gravity passive navigation could hold the navigator error to less than 20% of the requirement<sup>[5]</sup>. Although the function and performance of American's gravity passive navigation system are very strong, its price is very expensive. To produce a navigation system with

passive function and lower its cost, we put forward a kind of lower cost gravity passive navigation system, consisting of a gravity map and navigator with gravity measurement, i. e., a rate azimuth platform with a highly precise gravity sensor. In this paper we study the rate azimuth platform inertial navigation system and give the system navigation algorithm, error equations and its simulation results.

## 1 System Navigation Algorithm

The rate azimuth platform is a platform of two-ring type composed of a gyro stabilizer and gimbals. Two sets of one-degree-of-freedom integrated gyros, a one-degree-of-freedom rate gyro and three single axis accelerometers are mounted on the gyro stabilizer. In the inner stabilization axis, a pitching torque motor and a pose angular sensor are placed on its two ends respectively. On the ends of the outer stabilization axis, a rolling torque motor and a rolling pose sensor are arranged separately. Two integrated gyros and two accelerometers are used to measure and control the stabilization platform's turning, which makes the platform parallel with the local horizontal level. The definitions of coordinate frames are as follows. ① The local geodetic vertical (LGV) coordinate frame *OENU*. The origin is at the center of mass of the earth, *ON* axis is in the direction of geodetic north, *OE* axis is perpendicular to the meridian plane containing the vertical, directed toward the east, *OU* axis is directed outward along the local geodetic vertical. The geodetic vertical is everywhere normal to the reference ellipsoid. ② The local

Received 2004-10-20.

**Biography:** Cai Tijing (1961—), male, doctor, professor, caitij@seu.edu.cn.

level coordinate frame  $ox_n y_n z_n$ .  $oz_n$  axis is coincident with  $OU$  axis,  $ox_n$  and  $oy_n$  axes locate in the  $OEN$  plane and complete a right-handed system. In the navigational process the local level coordinate frame rotates about  $OU$  axis with an angular velocity  $-\dot{K}$  with respect to the coordinate frame  $OENU$ . If  $oy_n$  axis is coincident with the  $ON$  axis after calibration procedures, the azimuth angle of the local level coordinate frame is  $K$ , as shown in Fig. 1.

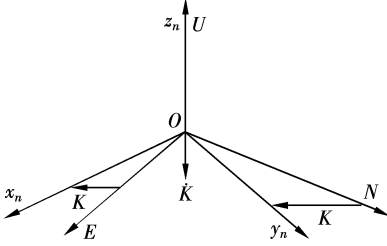


**Fig. 1** Local level coordinate frame  $ox_n y_n z_n$  and LGV coordinate frame  $OENU$

Under ideal conditions, gyro output  $\omega_n$  of RAP-INS is as follows:

$$\omega_n = C_h^m \omega_h - \begin{Bmatrix} 0 \\ 0 \\ \dot{K} \end{Bmatrix} \quad (1)$$

$$\text{where } C_h^m = \begin{bmatrix} \cos K & -\sin K & 0 \\ \sin K & \cos K & 0 \\ 0 & 0 & 1 \end{bmatrix}, \quad \omega_h = \{\omega_E, \omega_N, \omega_U\}^T,$$

$$\omega_E = -\dot{\varphi} = -\frac{V_N}{R_\varphi}, \quad \omega_N = (\Omega + \dot{\lambda}) \cos \varphi = \Omega \cos \varphi + \frac{V_E}{R_\lambda},$$

$$\omega_U = (\Omega + \dot{\lambda}) \sin \varphi = \Omega \sin \varphi + \frac{V_E}{R_\lambda} \tan \varphi, \quad \text{in which } \Omega \text{ is}$$

the earth angular velocity,  $\lambda$  is the geodetic longitude,  $\varphi$  is the geodetic latitude,  $V_E$  is east velocity,  $V_N$  is north velocity,  $R_\varphi$  and  $R_\lambda$  are radii of curvature of the earth reference ellipsoids in north-south and east-west directions, respectively.

Accelerometer output of RAPINS is given as follows:

$$\mathbf{a}_n = C_h^m \mathbf{a}_h \quad (2)$$

where  $\mathbf{a}_h = \{a_E, a_N, a_U\}^T$ ,  $a_E = \dot{V}_E + V_U(2\Omega + \dot{\lambda}) \cos \varphi - V_N(2\Omega + \dot{\lambda}) \sin \varphi - g_E$ ,  $a_N = \dot{V}_N + V_E(2\Omega + \dot{\lambda}) \sin \varphi + V_U \dot{\varphi} - g_N$ ,  $a_U = \dot{V}_U - V_E(2\Omega + \dot{\lambda}) \cos \varphi - V_N \dot{\varphi} - g_U$ , in which  $g_E$ ,  $g_N$  and  $g_U$  are the projections of gravity on the LGV coordinate frame  $OENU$ .

In practice, the computed velocities and geodetic longitude and latitude can be obtained by

$$V_{iC}(t) = V_i(t_0) + \int_{t_0}^t a_{iC}(\tau) d\tau \quad i = E, N, U \quad (3)$$

$$\varphi_C(t) = \varphi(t_0) + \int_{t_0}^t \frac{V_{NC}(\tau)}{R_\varphi(\tau)} d\tau \quad (4)$$

$$\lambda_C(t) = \lambda(t_0) + \int_{t_0}^t \frac{V_{EC}(\tau)}{R_\lambda(\tau) \cos \varphi(\tau)} d\tau \quad (5)$$

$$K_C = K(t_0) + \int_{t_0}^t \left( -\omega_{U0}(\tau) + \Omega \sin \varphi_C(\tau) + \frac{V_{EC}(\tau)}{R_\lambda(\tau)} \tan \varphi_C(\tau) \right) d\tau \quad (6)$$

where subscript C is used to designate computed value,  $a_{iC}$  is the computed acceleration and  $\omega_{U0}$  is practical output of rate azimuth gyro.

The platform commanded angular velocities are

$$\begin{Bmatrix} \omega_x \\ \omega_y \end{Bmatrix} = \begin{bmatrix} \cos K_C & -\sin K_C \\ \sin K_C & \cos K_C \end{bmatrix} \begin{Bmatrix} \omega_{EC} \\ \omega_{NC} \end{Bmatrix}$$

## 2 System Error Equations

Due to accelerometer and gyro inaccuracies and initial errors in platform alignment, the actual local level coordinate frame of the rate azimuth platform has small error angles  $\boldsymbol{\phi} = \{\phi_x, \phi_y, \phi_z\}^T$  with respect to its computed coordinate frame. Because the azimuth rate gyro is mounted on the two-axis platform,  $\phi_z = 0$ . Assuming that  $C_P^h$  and  $C_{PC}^h$  are the transformation matrices between the actual local level coordinate frame  $ox_n y_n z_n$  and the computed local level coordinate frame and the LGV coordinate frame  $OENU$ , their relationship is as follows:

$$C_P^h = C_{PC}^h C_P^{PC} \quad (7)$$

Letting the actual value equal the computed value minus the error and postmultiplying each side of Eq. (7) by  $C_h^P$ , we obtain

$$\boldsymbol{\phi}_h = C_n^h \boldsymbol{\phi} + \begin{Bmatrix} 0 \\ 0 \\ \Delta K \end{Bmatrix} \quad (8)$$

where  $\boldsymbol{\phi}_h = \{\phi_E, \phi_N, \phi_U\}^T$ . Calculating the derivative of each side of Eq. (8) and using equations  $\Delta \dot{K} = -\varepsilon_{zP} + \Delta \omega_{hC}$ ,  $\dot{C}_n^h = C_n^h \omega_n - C_n^h \omega_h$  and  $\dot{\boldsymbol{\phi}} = \omega_{PC} - \omega_n - \omega_n \boldsymbol{\phi} + \boldsymbol{\varepsilon}_P^{[5]}$ , we find attitude error equations:

$$\dot{\boldsymbol{\phi}}_h = -\omega_h \times \boldsymbol{\phi}_h + \Delta \omega_{hC} + C_n^h \boldsymbol{\varepsilon}_P - \begin{Bmatrix} 0 \\ 0 \\ \varepsilon_{zP} \end{Bmatrix} \quad (9)$$

where  $\Delta \omega_{hC} = \{\Delta \omega_{EC}, \Delta \omega_{NC}, \Delta \omega_{UC}\}^T$ ,  $\Delta \omega_{EC} = -\frac{1}{R}$

$$\Delta V_N, \quad \Delta \omega_{NC} = \frac{1}{R} \Delta V_E - \Omega \sin \varphi \Delta \varphi, \quad \Delta \omega_{UC} = \frac{1}{R}$$

$$\tan \varphi \Delta V_E + \left( \Omega \cos \varphi + \frac{V_E}{R \cos^2 \varphi} \right) \Delta \varphi, \quad \boldsymbol{\varepsilon}_P = \{\varepsilon_x, \varepsilon_y, 0\}^T,$$

$\varepsilon_{zP}$  is the drift of rate gyro, and  $R$  is the earth radius.

According to the definition of error we have the velocity error equations from Eq. (3):

$$\left. \begin{aligned} \Delta \dot{V}_E &= a_N \phi_U - a_U \phi_N + \delta a_E + \Delta a_{BE} - g_0 \eta_g \\ \Delta \dot{V}_N &= -a_E \phi_U + a_U \phi_E + \delta a_N + \Delta a_{BN} - g_0 \xi_g \\ \Delta \dot{V}_U &= a_E \phi_N - a_N \phi_E + \delta a_h + \Delta a_{Bh} + \Delta g \end{aligned} \right\} \quad (10)$$

where  $\delta a_E, \delta a_N$  and  $\delta a_U$  are the projections of accelerometer errors on the LGV coordinate frame  $OENU$ ,  $\xi_g$  and  $\eta_g$  are the deflections of the vertical,  $\Delta g$  is the gravity anomaly,  $g_0$  is the normal gravity.

$$\begin{aligned} \Delta a_{BE} &= -\Delta V_U(2\Omega + \dot{\lambda}) \cos \varphi + \Delta V_N(2\Omega + \dot{\lambda}) \sin \varphi + \\ &\quad \Delta \varphi [V_U(2\Omega + \dot{\lambda}) \sin \varphi + V_N(2\Omega + \dot{\lambda}) \cos \varphi] - \\ &\quad \left( \frac{\Delta V_E}{R \cos \varphi} + \Delta \varphi \frac{V_E \sin \varphi}{R \cos^2 \varphi} \right) (V_U \cos \varphi - V_N \sin \varphi) \\ \Delta a_{BN} &= -\Delta V_E(2\Omega + \dot{\lambda}) \sin \varphi - \Delta V_U \dot{\varphi} - \\ &\quad \Delta \varphi V_E(2\Omega + \dot{\lambda}) \cos \varphi - \frac{\Delta V_N}{R} V_U - \\ &\quad \left( \frac{\Delta V_E}{R \cos \varphi} + \Delta \varphi \frac{V_E \sin \varphi}{R \cos^2 \varphi} \right) V_E \sin \varphi \\ \Delta a_{BH} &= \Delta V_E(2\Omega + \dot{\lambda}) \cos \varphi + \Delta V_N 2\dot{\varphi} - \\ &\quad \Delta \varphi V_E(2\Omega + \dot{\lambda}) \sin \varphi + \\ &\quad \left( \frac{\Delta V_E}{R \cos \varphi} + \Delta \varphi \frac{V_E \sin \varphi}{R \cos^2 \varphi} \right) V_E \cos \varphi \end{aligned}$$

Position error equations can be obtained from Eqs. (4) and (5) according to the definition of error:

$$\left. \begin{aligned} \Delta \dot{\varphi} &= \frac{\Delta V_N}{R} \\ \Delta \dot{\lambda} &= \frac{\Delta V_E}{R \cos \varphi} + \frac{V_E \sin \varphi}{R \cos^2 \varphi} \Delta \varphi \\ \Delta \dot{h} &= \Delta V_U \end{aligned} \right\} \quad (11)$$

RAPINS is similar to three-axis platform inertial navigation system and its errors are mainly dependent on the stochastic errors of accelerometers and gyroscopes. Assume that random error models of accelerometer and gyro are as follows:

$$\begin{aligned} \delta_i &= \bar{\delta}_i + \delta_i^m + \tilde{\delta}_i, \quad \delta a_i = \delta \bar{a}_i + \delta \tilde{a}_i \\ \dot{\tilde{\delta}}_i &= \sqrt{Q_{gi}} \xi(t) \quad \tilde{\delta}_i(t_0) \\ \dot{\delta a_i} &= \sqrt{Q_{ai}} \xi(t) \quad \delta \tilde{a}_i(t_0) \\ \dot{\delta_i^m} &= -\mu_{\omega i} \delta_i^m + \sigma_{\omega i} \sqrt{2\mu_{\omega i}} \xi(t) \\ \tilde{\delta}_i &= \omega_i \Delta \bar{M}_{gi}, \quad \delta \tilde{a}_i = a_{bi} \Delta \bar{M}_{ai} \\ \Delta \dot{\bar{M}}_{gi} &= \sqrt{Q_{mi}} \xi(t) \quad \Delta \bar{M}_{gi}(t_0) \\ \Delta \dot{\bar{M}}_{ai} &= \sqrt{Q_{mi}} \xi(t) \quad \Delta \bar{M}_{ai}(t_0) \end{aligned}$$

where  $\bar{\delta}_i$  is the gyro bias drift,  $\delta_i^m$  is the gyro random walk,  $\tilde{\delta}_i$  is the gyro scale factor error,  $\omega_i$  is the gyro measure value,  $\Delta \bar{M}_{gi}$  is the gyro scale factor error,  $\delta \tilde{a}_i$  is the accelerometer bias,  $\Delta \bar{M}_{ai}$  is the accelerometer scale factor error, and  $a_{bi}$  is the accelerometer measure value.  $\bar{\delta}_i$ ,  $\delta_i^m$ , and  $\tilde{\delta}_i$  can be described by the Wiener

and Markov processes;  $\omega_i$ ,  $\Delta \bar{M}_{gi}$ ,  $\delta \tilde{a}_i$  and  $\Delta \bar{M}_{ai}$  can be described by the Wiener processes.

### 3 Simulation Results

Using the MATLAB/Simulink tools, we study the RAPINS and RAPINS with velocity damping. Let the vehicle with RAPINS have initial conditions and model parameters as follows: Initial position of longitude  $135^\circ$  and latitude  $30^\circ$ , initial velocity  $V_N = 20$  m/s,  $V_E = 0$ , RAP initial horizontal attitude (pitch and roll) error angles  $30''$ , azimuth error angle  $0.03^\circ$ , initial position and velocity error are zero, integrated gyro bias drift and random walk are  $0.05$  ( $^\circ$ )/h and  $0.01$  ( $^\circ$ )/h, rate gyro bias drift and random walk are  $0.1$  ( $^\circ$ )/h and  $1$  ( $^\circ$ )/h, respectively, scale factor error of gyro and accelerometer is  $0.3\%$ , three accelerometers biases are  $50$   $\mu$ g. Velocity damping is introduced in RAPINS by relative log. The mathematical model and parameters of relative log can be found in Ref. [6]. Fig. 2 shows the variability of attitude error angles of RAPINS with time. The pitch and roll error angles oscillate with the Schuler and the earth periods. The azimuth error angle is divergent slowly with time because of azimuth open-loop. The azimuth error angle depends on the performance of gyros, local geodetic latitude and motion form of vehicle. The curves of latitude and longitude errors of RAPINS are plotted in Fig. 3. The position error is about  $3$  nm/h. If the accuracy order of rate gyro is increased and the other conditions are not changed, the position error is improved and azimuth error angle distinctly decreases. Fig. 4 illustrates the curves of attitude error angles of RAPINS with velocity damping; horizontal attitude error angles are less than  $33''$ , azimuth error angle is less than  $7'$ . The Schuler and the earth oscillations are smoothed out. The variability of latitude and longitude errors of RAPINS with velocity damping with time is provided in Fig. 5. The position error is less than  $1$  130 m.

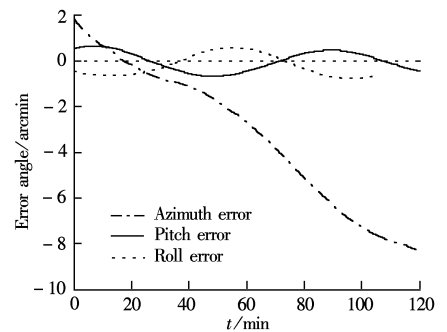


Fig. 2 Curves of the attitude error angles of RAPINS

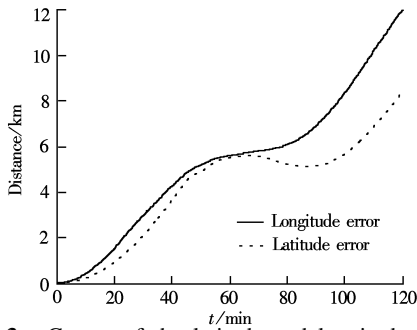


Fig. 3 Curves of the latitude and longitude errors of RAPINS

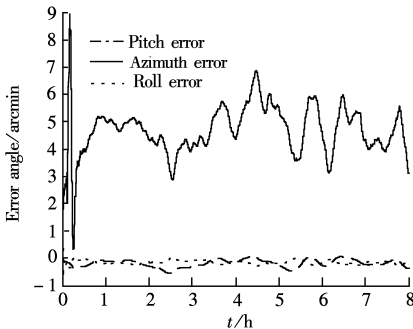


Fig. 4 Curves of the attitude error angles of RAPINS with velocity damping

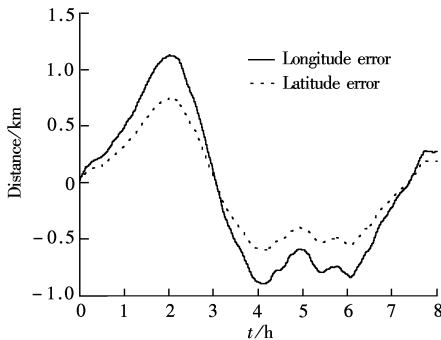


Fig. 5 Curves of the latitude and longitude errors of RAPINS with velocity damping

## 4 Conclusion

The rate azimuth platform inertial navigation system with velocity damping, consisting of medium precision accelerometers, rate integrating gyroscopes and lower precision rate gyroscope, and relative log, has small errors in platform attitude and position. If the system based on RAPINS contains a high accuracy gravity sensor put on the rate azimuth platform and the gravity map, it constitutes a lower cost gravity passive inertial navigation system.

## References

- [1] Ren Sicong. *Practical inertial navigation system principle* [M]. Beijing: Aerospace Press, 1988. 393 – 428. (in Chinese)
- [2] Liu Xihe, Hu Hengzhang, Song Youshan, et al. Application of accelerometers error model compensation in azimuth strapdown platform INS [J]. *Journal of Chinese Inertial Technology*, 1995, **3**(2): 48 – 52. (in Chinese)
- [3] Lowreys J A, Shellenbarger J C. Passive navigation using inertial navigation sensors and maps [J]. *Naval Engineers Journal*, 1997, **109**: 245 – 251.
- [4] Moryl J. Advanced submarine navigation systems [J]. *Sea Technology*, 1996, **37**(11): 33 – 39.
- [5] Rice Hugh, Mendelsohn Louis, Aarons Robert, et al. Next generation marine precision navigation system [A]. In: *IEEE 2000 Position Location and Navigation Symposium* [C]. New York: IEEE, Inc, 2000. 200 – 206.
- [6] Anuchin O N, Emeliantsev G I. *Integrated navigation system for sea moving objects*. 2nd Ed [M]. St. Petersburg: CSRI Electropribor, 2003. 110 – 181. (in Russian)

# 速率方位平台惯性导航系统研究

蔡体菁<sup>1</sup> 叶米里扬采夫<sup>2</sup>

(<sup>1</sup> 东南大学仪器科学与工程系, 南京 210096)

(<sup>2</sup> 圣彼得堡国立光机学院, 俄罗斯圣彼得堡 197101)

**摘要:** 为了降低重力无源导航系统成本, 在速率方位平台上放置一个重力敏感器, 以构成集重力仪和导航仪为一体的系统. 根据该系统的特点对速率方位平台惯性导航系统进行了研究, 给出了该系统的导航计算公式、速率方位平台姿态角、系统速度和位置的误差方程以及加速度计和陀螺仪的随机误差模型. 用 MATLAB/Simulink 工具对无阻尼和有阻尼速率方位平台惯性导航系统进行了计算机仿真, 仿真结果表明带阻尼的速率方位平台惯性导航系统平台误差角和定位误差小, 能够满足重力测量和导航要求.

**关键词:** 速率方位平台; 重力仪; 惯性导航系统; 重力无源导航系统

中图分类号: TN967.2